EUROPEAN ORGANIZATION FOR NUCLEAR RESEARCH (CERN)

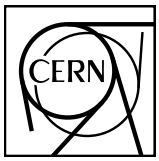

CERN-EP-2020-137
15 July 2020

# Search for the doubly heavy $\Xi_{bc}^0$ baryon via decays to $D^0pK^-$

LHCb collaboration[†]

**Abstract**

A search for the doubly heavy $\Xi_{bc}^0$ baryon using its decay to the $D^0pK^-$ final state is performed using proton-proton collision data at a centre-of-mass energy of 13 TeV collected by the LHCb experiment between 2016 and 2018, corresponding to an integrated luminosity of $5.4\,\text{fb}^{-1}$. No significant signal is found in the invariant mass range from 6.7 to 7.2 GeV/$c^2$. Upper limits are set at 95% credibility level on the ratio of the $\Xi_{bc}^0$ production cross-section times its branching fraction to $D^0pK^-$ relative to that of the $\Lambda_b^0 \to D^0pK^-$ decay. The limits are set as a function of the $\Xi_{bc}^0$ mass and lifetime hypotheses, in the rapidity range from 2.0 to 4.5 and in the transverse momentum region from 5 to 25 GeV/$c$. Upper limits range from $1.7 \times 10^{-2}$ to $3.0 \times 10^{-1}$ for the considered $\Xi_{bc}^0$ mass and lifetime hypotheses.

Submitted to JHEP



[†]Authors are listed at the end of this paper.

# 1 Introduction

In the constituent quark model [1,2], two heavy quarks ($b$ or $c$) can be bound together with a light quark to form doubly heavy baryons [3]. Studies of these particles are of great interest for the understanding of hadron spectroscopy and QCD at low energies. The $\Xi_{cc}^{++}$ baryon (valence quark content $ccu$)[1] was first observed in 2017 by the LHCb collaboration [4]. The $\Xi_{bc}^{0}$ baryon ($bcd$) containing two different heavy quarks is expected to have a mass in the range of $6.8 - 7.1\,\text{GeV}/c^2$ [5–19]. The $\Xi_{bc}^{0}$ production cross-section is predicted to be about 16 nb at a centre-of-mass energy of $\sqrt{s} = 13\,\text{TeV}$ in the pseudorapidity range $1.9 < \eta < 4.9$ and for a transverse momentum $p_{\text{T}} > 4\,\text{GeV}/c$ [20].

The $\Xi_{bc}^{0}$ baryon has not been observed to date. Five categories of $\Xi_{bc}^{0}$ decays have been studied theoretically: (i) semileptonic decays induced by $c \to d(s)\ell^+\nu_\ell$ or $b \to u(c)\ell^-\overline{\nu}_\ell$ transitions, with branching fractions estimated to be within the range $10^{-6} - 10^{-2}$ [21–26]; (ii) non-leptonic decays mediated by weak scattering of the $b$-quark and $c$-quark [12, 27]; (iii) non-leptonic decays occurring through $c$-quark charged current interaction, whose branching fractions are predicted to be $10^{-5} - 10^{-1}$ [22–26]; (iv) non-leptonic decays produced by $b$-quark charged current, with branching fractions ranging $10^{-9} - 10^{-3}$ [22–25, 28]; and (v) flavour-changing neutral current processes $b \to d(s)\ell^+\ell^-$, with branching fractions highly suppressed and within the range $10^{-10} - 10^{-8}$ [21, 29].

The $\Xi_{bc}^{0}$ lifetime is estimated by calculating full decay width which is expected to consist of four major contributions, due to $b \to cW^-$ and $c \to sW^+$ transitions, Pauli interference between the products of heavy quark decays and the quarks in the initial state, and weak scattering effects between the constituents, *e.g.* $bc \to cs$, $cd \to su$. The $\Xi_{bc}^{0}$ lifetime is predicted to be in the range of $90 - 280\,\text{fs}$ [12, 19, 30–32]. By contrast, Ref. [33] advocates that the $\Xi_{bc}^{0}$ lifetime is similar to that of the $B_c^+$ meson, *i.e.* $(510 \pm 9)\,\text{fs}$ [34].

This paper presents the first search for the $\Xi_{bc}^{0}$ baryon in the mass range from 6.7 to $7.2\,\text{GeV}/c^2$, using proton-proton ($pp$) collision data collected by the LHCb experiment at a centre-of-mass energy of $\sqrt{s} = 13\,\text{TeV}$ between 2016 and 2018, corresponding to an integrated luminosity of $5.4\,\text{fb}^{-1}$. The $\Xi_{bc}^{0}$ baryon is searched for through the $\Xi_{bc}^{0} \to D^0 p K^-$, $D^0 \to K^-\pi^+$ decay chain, which is preferred for its ease of reconstruction at LHCb. A leading-order Feynman diagram contributing to this decay is shown in Fig. 1. The branching fraction $\mathcal{B}(\Xi_{bc}^{0} \to D^0 p K^-)$ is expected to be similar to that of the $\Xi_{bc}^{+} \to D^0 p K^0$ decay, about 0.1% [12]. Considering the value of $\mathcal{B}(D^0 \to K^-\pi^+) = (3.89 \pm 0.04)\%$ [34], the total branching fraction of the $\Xi_{bc}^{0} \to D^0(\to K^-\pi^+)pK^-$ decay chain is expected to be in the range of $10^{-5} - 10^{-4}$.

To reduce systematic uncertainties, the $\Xi_{bc}^{0}$ production cross-section is measured relative to that of the normalisation mode corresponding to a $\Lambda_b^0$ baryon decaying to the same final state. Both the $\Xi_{bc}^{0}$ and $\Lambda_b^0$ baryons are reconstructed in the rapidity range from 2.0 to 4.5 and in the transverse momentum region from 5 to $25\,\text{GeV}/c$. The search is performed with the analysis procedure entirely defined before inspecting the data across the considered mass range.

[1] The inclusion of charge-conjugate modes is implied throughout this paper.

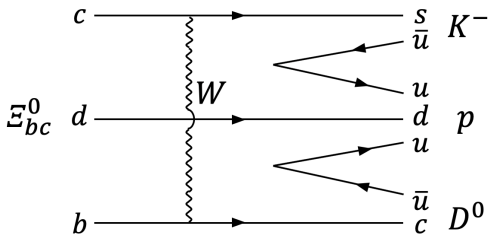


Figure 1: The $\Xi_{bc}^0 \to D^0 p K^-$ decay induced by the weak $W$-scattering of constituent $b$ and $c$ quarks.

# 2 Detector and simulation

The LHCb detector [35, 36] is a single-arm forward spectrometer covering the pseudorapidity range $2 < \eta < 5$, designed for the study of particles containing $b$ or $c$ quarks. The detector includes a high-precision tracking system consisting of a silicon-strip vertex detector surrounding the $pp$ interaction region [37], a large-area silicon-strip detector located upstream of a dipole magnet with a bending power of about 4 Tm, and three stations of silicon-strip detectors and straw drift tubes [38] placed downstream of the magnet. The polarity of the dipole magnet is reversed periodically throughout data taking. The tracking system provides a measurement of the momentum, $p$, of charged particles with a relative uncertainty that varies from 0.5% at low momentum to 1.0% at 200 GeV/$c$. The minimum distance of a track to a primary $pp$ interaction vertex (PV), the impact parameter (IP), is measured with a resolution of $(15 + 29/p_{\rm T})\,\mu$m, where $p_{\rm T}$ is expressed in GeV/$c$. Different types of charged hadrons are distinguished using information from two ring-imaging Cherenkov detectors [39]. Photons, electrons and hadrons are identified by a calorimeter system consisting of scintillating-pad and preshower detectors, an electromagnetic and a hadronic calorimeter. Muons are identified by a system composed of alternating layers of iron and multiwire proportional chambers [40]. The online event selection is performed by a trigger [41], which consists of a hardware stage, based on information from the calorimeters and muon systems [42], followed by a software stage, at which all tracks with $p_{\rm T} > 300\,$MeV/$c$ are reconstructed for data collected at $\sqrt{s} = 13\,$TeV [43]. The software trigger used in this analysis requires a two-, three- or four-track vertex with significant displacement from any PV. At least one charged particle must have $p_{\rm T} > 1.7\,$GeV/$c$ and be inconsistent with originating from any PV. A multivariate algorithm [44] is used for the identification of displaced vertices consistent with the decay of a $b$ hadron.

Simulated samples are used to develop the candidate selection and to estimate the corresponding efficiency as well as that of the detector acceptance. Simulated $pp$ collisions are generated using Pythia [45] with a specific LHCb configuration [46]. A dedicated

package, GenXicc2.0 [47], is used to simulate the $\Xi_{bc}^0$ baryon production. Decays of unstable particles are described by EvtGen [48], in which final-state radiation is generated using Photos [49]. The interaction of the generated particles with the detector, and its response, are simulated using the Geant4 toolkit [50] as described in Ref. [51]. The simulated $\Xi_{bc}^0$ events are generated with a mass of $6.9\,\text{GeV}/c^2$ and a lifetime of 400 fs, and samples with different mass and lifetime hypotheses are obtained using a weighting technique. The $\Xi_{bc}^0$ baryon decay is assumed to follow a uniform phase-space model.

# 3 Reconstruction and selection

For both the $\Xi_{bc}^0$ signal and the $\Lambda_b^0$ normalisation modes, $D^0$ candidates are reconstructed in the $K^-\pi^+$ final state. Two oppositely charged tracks identified as a kaon and a pion with an invariant mass in the range of $1.84 < m(K^-\pi^+) < 1.89\,\text{GeV}/c^2$ are requested to form a common vertex that is significantly displaced from any PV. The $D^0$ candidate is then combined with two oppositely charged tracks identified as a proton and as a kaon to form a $\Xi_{bc}^0$ or a $\Lambda_b^0$ candidate. The two tracks are required to have a high transverse momentum and to be inconsistent with originating from any PV. The $D^0$, $p$ and $K$ candidates are required to form a common vertex with a good fit quality. The $\Xi_{bc}^0$ and $\Lambda_b^0$ candidates have to point back to the PV and have an invariant mass larger than $5.0\,\text{GeV}/c^2$.

A multivariate analysis is applied to both the signal and the normalisation candidates to further improve the purity of the samples. The selection algorithm is a Boosted Decision Tree (BDT) algorithm implemented in the TMVA package [52]. To train this classifier, simulated $\Xi_{bc}^0$ baryon decays are used as the signal proxy and candidates lying in the upper $D^0pK^-$ mass sideband ($8.0 - 8.5\,\text{GeV}/c^2$) adjacent to the signal region for the background proxy. The BDT algorithm uses kinematic and vertex-topology variables that show good discrimination power between signal and background. The variables include: the $\chi^2_{\text{IP}}$ and transverse momentum of all particles; particle identification (PID) variables for the final state particles; the flight-distance $\chi^2$ between the PV and the decay vertex; the vertex quality of the $D^0$ and $\Xi_{bc}^0$ candidates; and the angle between the momentum and the flight direction of the $\Xi_{bc}^0$ candidate. The $\chi^2_{\text{IP}}$ is defined as the difference in $\chi^2$ of the PV fit with and without the particle in question. The flight-distance $\chi^2$ is defined as the $\chi^2$ of the hypothesis that the decay vertex of the candidate coincides with its associated PV, defined as the PV with the smallest $\chi^2_{\text{IP}}$. It has been verified that this BDT classifier does not shape the background invariant mass distribution.

A selection requirement is applied on the BDT response. It is determined by maximizing the value of the Punzi figure of merit $\varepsilon/(\frac{a}{2} + \sqrt{N_B})$ [53], where $\varepsilon$ is the estimated signal efficiency, $a$ corresponds to the number of standard deviations in a Gaussian significance test, which is taken as 5, and $N_B$ is the number of background candidates determined in the upper sideband and extrapolated to the signal region. The performance of the BDT classifier is tested and found to be stable against the $\Xi_{bc}^0$ lifetime in the range from 100 to 500 fs.

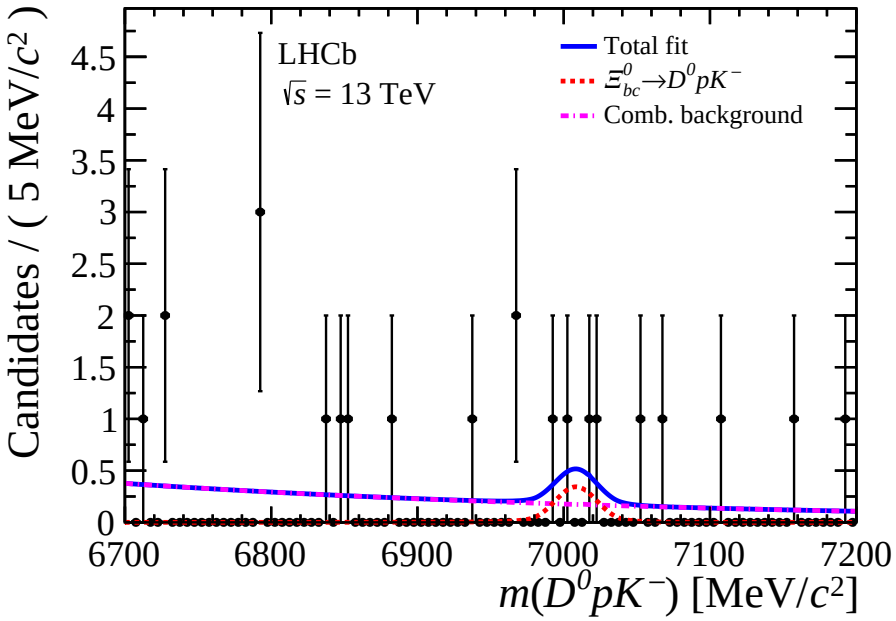


Figure 2: Invariant mass $m(D^0pK^-)$ distribution of selected $\Xi_{bc}^0$ candidates (black points) together with the projection of the fit (blue solid line) for the full data sample. The $\Xi_{bc}^0 \to D^0pK^-$ signal component, with the central mass value varying freely (red dashed line), and combinatorial background (purple dotted line) are also shown.

# 4 Yield measurements

The invariant mass distribution of the selected candidates within the range $6.7-7.2\,\text{GeV}/c^2$ for the full data sample is shown in Fig. 2. The $\Xi_{bc}^0$ signal yield is determined from an unbinned maximum likelihood fit to the invariant mass $m(D^0pK^-)$ distribution. The signal is described by a double-sided Crystal Ball (DSCB) function [54] comprising a Gaussian core with power-law tails on both sides, while the background is described by an exponential function. The parameters of the signal model are fixed from simulation except for the peak position that is allowed to vary in the fit. The mass resolution of the signal decay is $14.2 \pm 0.4\,\text{MeV}/c^2$ for all mass hypotheses, as determined from simulation. The projection of the fit to the mass distribution, with the $\Xi_{bc}^0$ mass parameter varying freely, is also shown in Fig. 2. No excess is observed in the full $\Xi_{bc}^0$ mass range, therefore upper limits are set on the production ratios.

As the selection efficiency varies with the data-taking conditions, the yield of the normalisation mode is determined for each year separately. The $\Lambda_b^0$ signal yield, $N_{\text{norm}}$, is obtained from an extended unbinned maximum-likelihood fit to the invariant mass $m(D^0pK^-)$ distribution in the 2016, 2017 and 2018 data samples. The fit model includes a DSCB function to describe the $\Lambda_b^0 \to D^0pK^-$ decay and three separate background components: random combinations of tracks or genuine $D^0$ decays combined with random tracks (combinatorial background); the Cabibbo-favoured decay $\Lambda_b^0 \to D^0p\pi^-$ where the pion is incorrectly identified as a kaon (misidentified background); and the $\Xi_b^0 \to D^0pK^-$ decay component. The shape of the normalisation mode and the misidentified background are taken from simulation. The latter is parameterised with a Crystal Ball (CB) function. The $\Xi_b^0 \to D^0pK^-$ decay component is described by a DSCB function and the

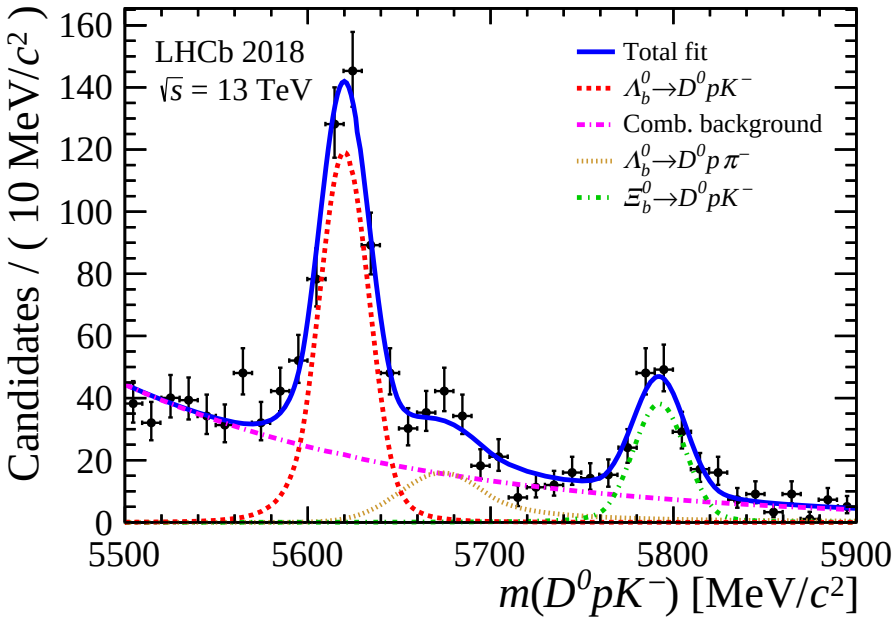


Figure 3: Invariant mass distribution for $\Lambda_b^0 \to D^0 pK^-$ candidates in the 2018 data sample (black points). The fit projection (blue solid line) is superimposed. The normalisation component (red dashed line), the misidentified background (brown dashed line), the combinatorial background (purple dotted line), and the $\Xi_b^0 \to D^0 pK^-$ (green dotted line) components are also shown. Similar distributions are obtained for the 2016 and 2017 data samples.

combinatorial background by an exponential function. As an illustration, the $m(D^0pK^-)$ distribution for the 2018 data sample is shown in Fig. 3 along with the projection of the associated fit result. A total of about 1200 $\Lambda_b^0$ candidates are obtained.

# 5 Production cross-section ratio

The production cross-section ratio, $R$, is defined as

$$R \equiv \frac{\sigma(\Xi_{bc}^0)\mathcal{B}(\Xi_{bc}^0 \to D^0pK^-)}{\sigma(\Lambda_b^0)\mathcal{B}(\Lambda_b^0 \to D^0pK^-)} = \frac{\epsilon_{\rm norm}}{\epsilon_{\rm sig}} \frac{N_{\rm sig}}{N_{\rm norm}} \equiv \alpha N_{\rm sig}, \tag{1}$$

where $\sigma$ is the production cross-section and $\mathcal{B}$ is the decay branching fraction, $\epsilon_{\rm sig}$ and $\epsilon_{\rm norm}$ are the selection efficiencies of the signal and normalisation decay modes, respectively, $N_{\rm sig}$ and $N_{\rm norm}$ are the corresponding yields, and $\alpha = \epsilon_{\rm norm}/(\epsilon_{\rm sig} N_{\rm norm})$ is the single-event sensitivity.

The signal efficiency depends upon the assumed mass and lifetime of the $\Xi_{bc}^0$. Simulated events are generated with $m(\Xi_{bc}^0) = 6.9\,{\rm GeV}/c^2$ and $\tau(\Xi_{bc}^0) = 400\,{\rm fs}$, from here on referred to as nominal, and used to evaluate the efficiency ratio. The variation of the efficiency ratio as a function of $m(\Xi_{bc}^0)$ and $\tau(\Xi_{bc}^0)$ relative to the nominal point is then determined with a weighting technique discussed in Sec. 7. The kinematic distribution of $\Xi_{bc}^0$ baryons produced at the LHC is also unknown and is assumed to be the same as for the $\Lambda_b^0$ baryon. Transverse momentum and rapidity distributions of simulated $\Xi_{bc}^0$ are therefore corrected to match that of $\Lambda_b^0$ decays observed in data.

The efficiencies can be factorised into that of the geometrical acceptance, track reconstruction, trigger, offline pre-selection, PID, and multivariate selection. The individual efficiencies are evaluated with simulated events of $\Xi_{bc}^0 \to D^0 p K^-$ and $\Lambda_b^0 \to D^0 p K^-$ decays, except for tracking and PID where the efficiencies are determined using calibration data samples, namely the $J/\psi \to \mu^+\mu^-$ decay [55] for tracking and $D^{*+} \to D^0 (\to K^-\pi^+)\pi^+$ and $\Lambda \to p\pi^-$ decays for PID [56, 57].

The track multiplicity distribution is taken from $\Lambda_b^0 \to D^0 p K^-$ data for both signal and normalisation samples. The simulated Dalitz plot of these decays are corrected to match the distribution observed in background-subtracted data, obtained using the *sPlot* technique [58]. The efficiency ratio and the single-event sensitivity at the nominal $\Xi_{bc}^0$ mass and lifetime are summarised in Table 1. The single-event sensitivity is determined according to Eq. (1) using the obtained efficiency ratios and the normalisation yields reported in Table 1.

The analysis is performed assuming a uniform phase-space model for the signal decay $\Xi_{bc}^0 \to D^0 p K^-$. Efficiency maps in bins of the invariant masses $m(D^0 p)$ and $m(pK^-)$ are provided in Fig. 4 to allow for the interpretation of the result in different theoretical model scenarios.

# 6 Systematic uncertainties

Systematic uncertainties on the production ratio arise from the fit model, the trigger efficiency, the PID efficiency, the Dalitz plot weighting, and the simulation and data difference. The total systematic uncertainty is calculated as the quadratic sum of the individual uncertainties, presented in Table 2, assuming all the sources are uncorrelated.

The uncertainty on the signal yield may arise from the shape of the signal, the combinatorial background, and the misidentified background. This is quantified by choosing alternative functions. A Gaussian function is used for the signal and a second-order polynomial for the combinatorial background. The effect due to the misidentified background is estimated by fixing the ratio of the $\Lambda_b^0 \to D^0 p\pi^-$ yield to that of the $\Lambda_b^0 \to D^0 p K^-$ decay with their measured branching fractions [59], taking into account their selection efficiencies. The sum in quadrature of these uncertainty estimates, yielding 3.6%, is taken as systematic uncertainty due to the fit model.

The cancellation of the hardware-trigger efficiencies in the ratio between the signal and the normalisation modes is studied with $B^0 \to \overline{D}^0\pi^+\pi^-$ control samples, using a tag-and-probe method [60]. The data and simulation difference between the efficiency ratio in the normalisation mode $\Lambda_b^0 \to D^0 p K^-$ and the $B^0 \to \overline{D}^0\pi^+\pi^-$ control sample is

Table 1: Efficiency ratios between the normalisation and signal modes and the single-event sensitivity, $\alpha$, for the nominal $\Xi_{bc}^0$ hypothesis, $m(\Xi_{bc}^0) = 6.9\,\text{GeV}/c^2$ and $\tau(\Xi_{bc}^0) = 400\,\text{fs}$. The uncertainties are statistical only.

| Period | $\epsilon_{\text{norm}}/\epsilon_{\text{sig}}$ | $N_{\text{norm}}$ | $\alpha$ $[\times 10^{-3}]$ |
|---|---|---|---|
| 2016 | $3.66 \pm 0.17$ | $376 \pm 26$ | $9.7 \pm 0.8$ |
| 2017 | $3.50 \pm 0.13$ | $371 \pm 26$ | $9.4 \pm 0.7$ |
| 2018 | $3.22 \pm 0.13$ | $425 \pm 28$ | $7.6 \pm 0.6$ |

Table 2: Summary of the systematic uncertainties on measurement of the production ratio, $R$.

| Source | $R$ [%] |
|---|---|
| Fit model | 3.6 |
| Hardware trigger | 6.8 |
| PID | 5.4 |
| $\Lambda_b^0 \to D^0 p K^-$ Dalitz plot weight | 1.5 |
| Simulation/data difference | 5.0 |
| Total | 10.7 |

assigned as a systematic uncertainty, and amounts to 6.8%.

The PID efficiency is determined in bins of particle momentum and pseudorapidity using calibration data samples. There are several associated sources of systematic uncertainty, namely due to the limited size of the control samples, notably for high-$p_{\mathrm{T}}$ protons from the $\Lambda$ sample, the assumption that kinematic correlations between tracks are neglected, and limitations in the method (*e.g.* the finite kinematic binning used). The total systematic uncertainty associated with the PID efficiency, calculated as the sum in quadrature of individual contributions, amounts to 5.4%.

The Dalitz plot of the simulated $\Lambda_b^0 \to D^0 p K^-$ decays is weighted to match that observed in data. Several binning schemes of the Dalitz plot have been considered and the maximal difference in $R$ of 1.5% is taken as the corresponding systematic uncertainty.

The simulation and data agreement is checked with control modes, and a difference of 5.0% is found between different years of data-taking, which is taken as systematic uncertainty.

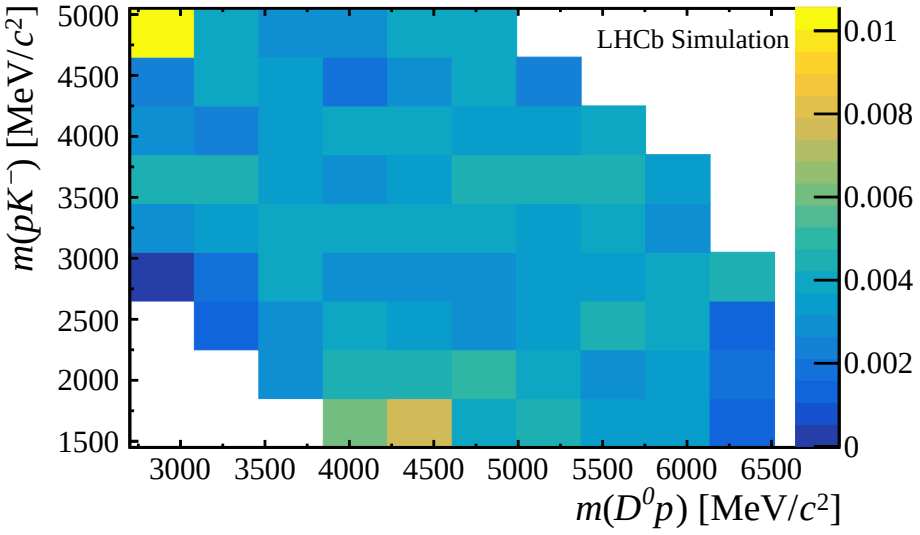


Figure 4: Efficiency of selected $\Xi_{bc}^0 \to D^0 p K^-$ decays as a function of the invariant masses $m(D^0 p)$ and $m(pK^-)$ in the simulation. The variation of efficiency across the Dalitz plot reflects the specific phase-space dependent requirements of the selection.

Table 3: Single-event sensitivity $\alpha$ in units of $10^{-3}$ for different lifetime hypotheses of the $\Xi_{bc}^0$ baryon for different data-taking periods. The uncertainties are due to the limited size of the simulated samples and the statistical uncertainties on the measured $\Lambda_b^0$ baryon yields.

| Period | $\tau = 100\,\text{fs}$ | $\tau = 200\,\text{fs}$ | $\tau = 300\,\text{fs}$ | $\tau = 400\,\text{fs}$ | $\tau = 500\,\text{fs}$ |
|---|---|---|---|---|---|
| 2016 | $141 \pm 14$ | $27.5 \pm 2.4$ | $14.1 \pm 1.2$ | $9.7 \pm 0.8$ | $7.7 \pm 0.7$ |
| 2017 | $134 \pm 12$ | $25.9 \pm 2.1$ | $13.5 \pm 1.1$ | $9.5 \pm 0.8$ | $7.6 \pm 0.6$ |
| 2018 | $102 \pm 9$ | $20.8 \pm 1.6$ | $10.8 \pm 0.8$ | $7.6 \pm 0.6$ | $6.1 \pm 0.5$ |

# 7 Variation of efficiency with mass and lifetime

The trigger, reconstruction and selection efficiencies for $\Xi_{bc}^0$ candidates have a strong dependence upon the $\Xi_{bc}^0$ lifetime. The simulated $\Xi_{bc}^0$ events are generated with a lifetime value of 400 fs. To test other lifetime hypotheses, the simulated events are weighted to reproduce other lifetime hypotheses and the efficiency is recalculated. A discrete set of hypotheses (100, 200, 300, 400 and 500 fs) is considered. The value and uncertainty on the single-event sensitivity $\alpha$ are provided for each lifetime hypothesis in Table 3.

The efficiency could also depend on the $\Xi_{bc}^0$ baryon mass hypothesis in the simulation, since it affects the kinematic distributions of the decay products. To assess its effect, large samples of simulated events are generated with alternative mass hypotheses, namely 6.7 and 7.1 GeV/$c^2$. The efficiencies for other mass values are interpolated between the nominal and these two hypotheses. Two tests are carried out with these samples. Firstly, the detector acceptance efficiency is recomputed. Secondly, the $p_{\text{T}}$ distributions of the $\Xi_{bc}^0$ baryon daughters are weighted to match those of the alternative mass hypothesis and the remaining efficiency is recalculated. The total efficiency is found to have negligible dependence on the $\Xi_{bc}^0$ mass, thus it is ignored in the evaluation of the single-event sensitivities.

# 8 Results

The upper limits on the $\Xi_{bc}^0$ decay ratio $R$ are obtained by performing again a fit to the data invariant mass distribution assuming different $\Xi_{bc}^0$ mass hypotheses in the range from 6.7 to 7.2 GeV/$c^2$, and in steps of 7.5 MeV/$c^2$, for five lifetime hypotheses, in the fiducial region of rapidity $2.0 < y < 4.5$ and transverse momentum $5 < p_{\text{T}} < 25\,\text{GeV}/c$. For each $\Xi_{bc}^0$ baryon mass and lifetime hypothesis, the likelihood profile $\mathcal{L}(R)$ is determined as a function of $R$ with simultaneous fits to the $m(D^0pK^-)$ invariant mass distributions. Then it is convoluted with a Gaussian distribution whose width is a quadratic sum of the statistical and systematic uncertainty on the single-event sensitivity. The upper limit at 95% credibility level (CL) is defined as the value of $R$ at which the integral of the profile likelihood equals 95% of its total area. Upper limits on $R$ at 95% CL for different lifetime hypotheses are shown in Fig. 5.

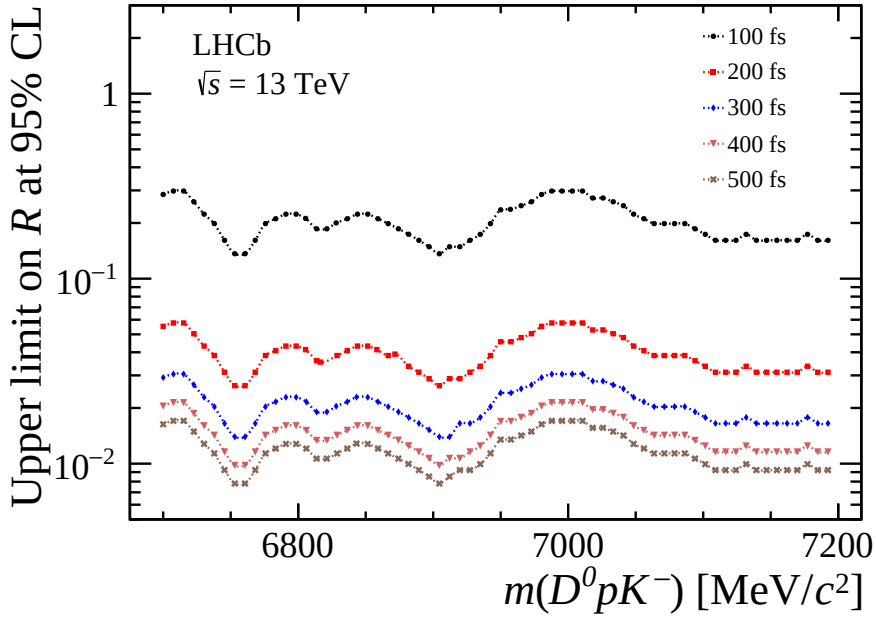


Figure 5: Values of upper limits on $R$ at 95% CL as a function of $m(D^0pK^-)$ for five $\Xi_{bc}^0$ lifetime hypotheses. The curves from top to bottom correspond to lifetime hypotheses from 100 fs to 500 fs, respectively.

# 9 Conclusion

A first search for the $\Xi_{bc}^0 \to D^0pK^-$ decay is performed at LHCb with a data sample of $pp$ collisions, corresponding to an integrated luminosity of $5.4\,\text{fb}^{-1}$, recorded at a centre-of-mass energy of 13 TeV. No evidence for a signal is found. Upper limits at 95% CL on the $\Xi_{bc}^0$ baryon production cross-section times its branching fraction to the $D^0pK^-$ final state relative to the $\Lambda_b^0 \to D^0pK^-$ decay are obtained in the fiducial region of rapidity $2.0 < y < 4.5$ and transverse momentum $5 < p_{\rm T} < 25\,\text{GeV}/c$, and for various $\Xi_{bc}^0$ mass and lifetime hypotheses. The upper limits are set assuming that the kinematic distributions of the $\Xi_{bc}^0$ baryon follow those of the GenXicc2.0 model [47] and that the decay of the $\Xi_{bc}^0$ baryon proceeds according to a uniform phase-space model. The values of the upper limits depend strongly on the lifetime, varying from $3.0 \times 10^{-1}$ to $1.7 \times 10^{-2}$ for 100 fs and 500 fs, respectively. Future searches at LHCb with improved trigger conditions, additional $\Xi_{bc}^0$ decay modes, and larger data samples will further improve the $\Xi_{bc}^0$ signal sensitivity.

# Acknowledgements

We thank Chao-Hsi Chang, Cai-Dian Lü, Wei Wang, Xing-Gang Wu, and Fu-Sheng Yu for frequent and interesting discussions on the production and decays of double-heavy-flavor baryons. We express our gratitude to our colleagues in the CERN accelerator departments for the excellent performance of the LHC. We thank the technical and administrative staff at the LHCb institutes. We acknowledge support from CERN and from the national agencies: CAPES, CNPq, FAPERJ and FINEP (Brazil); MOST and NSFC (China); CNRS/IN2P3 (France); BMBF, DFG and MPG (Germany); INFN

(Italy); NWO (Netherlands); MNiSW and NCN (Poland); MEN/IFA (Romania); MSHE (Russia); MinECo (Spain); SNSF and SER (Switzerland); NASU (Ukraine); STFC (United Kingdom); DOE NP and NSF (USA). We acknowledge the computing resources that are provided by CERN, IN2P3 (France), KIT and DESY (Germany), INFN (Italy), SURF (Netherlands), PIC (Spain), GridPP (United Kingdom), RRCKI and Yandex LLC (Russia), CSCS (Switzerland), IFIN-HH (Romania), CBPF (Brazil), PL-GRID (Poland) and OSC (USA). We are indebted to the communities behind the multiple open-source software packages on which we depend. Individual groups or members have received support from AvH Foundation (Germany); EPLANET, Marie Skłodowska-Curie Actions and ERC (European Union); A*MIDEX, ANR, Labex P2IO and OCEVU, and Région Auvergne-Rhône-Alpes (France); Key Research Program of Frontier Sciences of CAS, CAS PIFI, and the Thousand Talents Program (China); RFBR, RSF and Yandex LLC (Russia); GVA, XuntaGal and GENCAT (Spain); the Royal Society and the Leverhulme Trust (United Kingdom).

# References

[1] M. Gell-Mann, *A Schematic Model of Baryons and Mesons*, Phys. Lett. **8** (1964) 214.

[2] G. Zweig, *An $SU_3$ model for strong interaction symmetry and its breaking; Version 1*, Tech. Rep. CERN-TH-401, CERN, Geneva, 1964; G. Zweig, *An $SU_3$ model for strong interaction symmetry and its breaking; Version 2*, .

[3] S. Fleck, B. Silvestre-Brac, and J.-M. Richard, *Search for diquark clustering in baryons*, Phys. Rev. **D38** (1988) 1519.

[4] LHCb collaboration, R. Aaij *et al.*, *Observation of the doubly charmed baryon $\Xi_{cc}^{++}$*, Phys. Rev. Lett. **119** (2017) 112001, arXiv:1707.01621.

[5] D. Ebert, R. N. Faustov, V. O. Galkin, and A. P. Martynenko, *Mass spectra of doubly heavy baryons in the relativistic quark model*, Phys. Rev. **D66** (2002) 014008, arXiv:hep-ph/0201217.

[6] S. S. Gershtein, V. V. Kiselev, A. K. Likhoded, and A. I. Onishchenko, *Spectroscopy of doubly heavy baryons*, Phys. Rev. **D62** (2000) 054021.

[7] D. Ebert *et al.*, *Heavy baryons in the relativistic quark model*, Z. Phys. **C76** (1997) 111, arXiv:hep-ph/9607314.

[8] R. Roncaglia, A. Dzierba, D. B. Lichtenberg, and E. Predazzi, *Predicting the masses of heavy hadrons without an explicit Hamiltonian*, Phys. Rev. **D51** (1995) 1248, arXiv:hep-ph/9405392.

[9] I. M. Narodetskii and M. A. Trusov, *The doubly heavy baryons in the nonperturbative QCD approach*, Baryons 2002 (2003) 639, arXiv:hep-ph/0204320.

[10] R. Roncaglia, D. B. Lichtenberg, and E. Predazzi, *Predicting the masses of baryons containing one or two heavy quarks*, Phys. Rev. **D52** (1995) 1722, arXiv:hep-ph/9502251.

[11] D. B. Lichtenberg, R. Roncaglia, and E. Predazzi, *Mass sum rules for singly and doubly heavy flavored hadrons*, Phys. Rev. **D53** (1996) 6678, arXiv:hep-ph/9511461.

[12] V. V. Kiselev and A. K. Likhoded, *Baryons with two heavy quarks*, Phys. Usp. **45** (2002) 455, arXiv:hep-ph/0103169.

[13] D.-H. He *et al.*, *Evaluation of spectra of baryons containing two heavy quarks in bag model*, Phys. Rev. **D70** (2004) 094004, arXiv:hep-ph/0403301.

[14] C. Albertus, E. Hernandez, J. Nieves, and J. M. Verde-Velasco, *Static properties and semileptonic decays of doubly heavy baryons in a nonrelativistic quark model*, Eur. Phys. J. **A32** (2007) 183, arXiv:hep-ph/0610030, [Erratum: Eur.Phys.J.A 36, 119 (2008)].

[15] W. Roberts and M. Pervin, *Heavy baryons in a quark model*, Int. J. Mod. Phys. **A23** (2008) 2817, arXiv:0711.2492.

[16] S. M. Gerasyuta and E. E. Matskevich, *S-wave bottom baryons*, Int. J. Mod. Phys. **E18** (2009) 1785, arXiv:0803.3497.

[17] M.-H. Weng, X.-H. Guo, and A. W. Thomas, *Bethe-Salpeter equation for doubly heavy baryons in the covariant instantaneous approximation*, Phys. Rev. **D83** (2011) 056006, arXiv:1012.0082.

[18] J.-R. Zhang and M.-Q. Huang, *Doubly heavy baryons in QCD sum rules*, Phys. Rev. **D78** (2008) 094007, arXiv:0810.5396.

[19] M. Karliner and J. L. Rosner, *Baryons with two heavy quarks: Masses, production, decays, and detection*, Phys. Rev. **D90** (2014) 094007, arXiv:1408.5877.

[20] J.-W. Zhang *et al.*, *Hadronic production of the doubly heavy baryon $\Xi_{bc}$ at LHC*, Phys. Rev. **D83** (2011) 034026, arXiv:1101.1130.

[21] X.-H. Hu, R.-H. Li, and Z.-P. Xing, *A comprehensive analysis of weak transition form factors for doubly heavy baryons in the light front approach*, Eur. Phys. J. **C80** (2020) 320, arXiv:2001.06375.

[22] Y.-J. Shi, W. Wang, and Z.-X. Zhao, *QCD Sum Rules Analysis of Weak Decays of Doubly-Heavy Baryons*, Eur. Phys. J. C **80** (2020) 568, arXiv:1902.01092.

[23] W. Wang, F.-S. Yu, and Z.-X. Zhao, *Weak decays of doubly heavy baryons: the $1/2 \to 1/2$ case*, Eur. Phys. J. **C77** (2017) 781, arXiv:1707.02834.

[24] A. S. Gerasimov and A. V. Luchinsky, *Weak decays of doubly heavy baryons: Decays to a system of $\pi$ mesons*, Phys. Rev. **D100** (2019) 073015, arXiv:1905.11740.

[25] Z.-X. Zhao, *Weak decays of doubly heavy baryons: the $1/2 \to 3/2$ case*, Eur. Phys. J. **C78** (2018) 756, arXiv:1805.10878.

[26] A. V. Berezhnoy, A. K. Likhoded, and A. V. Luchinsky, *Doubly heavy baryons at the LHC*, Phys. Rev. **D98** (2018) 113004, arXiv:1809.10058.

[27] R.-H. Li *et al.*, *Doubly-heavy baryon weak decays: $\Xi_{bc}^0 \to pK^-$ and $\Xi_{cc}^+ \to \Sigma_c^{++}(2520)K^-$*, Phys. Lett. **B767** (2017) 232, arXiv:1701.03284.

[28] V. V. Kiselev and O. P. Yushchenko, *Possibility of measuring the CP-violation $\gamma$-parameter in decays of $\Xi_{bc}$ baryons*, Phys. Lett. **B568** (2003) 219, arXiv:hep-ph/0211382.

[29] Z.-P. Xing and Z.-X. Zhao, *Weak decays of doubly heavy baryons: the FCNC processes*, Phys. Rev. **D98** (2018) 056002, arXiv:1807.03101.

[30] H.-Y. Cheng and F. Xu, *Lifetimes of doubly heavy baryons $\mathcal{B}_{bb}$ and $\mathcal{B}_{bc}$*, Phys. Rev. **D99** (2019) 073006, arXiv:1903.08148.

[31] V. V. Kiselev, A. K. Likhoded, and A. I. Onishchenko, *Lifetimes of $\Xi_{bc}^+$ and $\Xi_{bc}^0$ baryons*, Eur. Phys. J. **C16** (2000) 461, arXiv:hep-ph/9901224.

[32] J. D. Bjorken, *Estimates of decay branching ratios for hadrons containing charm and bottom quarks.*, Tech. Rep. FERMILAB-PUB-86-189-T, 1986.

[33] M. A. Sanchis-Lozano, *Weak decays of doubly heavy hadrons*, Nucl. Phys. **B440** (1995) 251, arXiv:hep-ph/9502359.

[34] Particle Data Group, M. Tanabashi *et al.*, *Review of particle physics*, Phys. Rev. **D98** (2018) 030001, and 2019 update.

[35] LHCb collaboration, A. A. Alves Jr. *et al.*, *The LHCb detector at the LHC*, JINST **3** (2008) S08005.

[36] LHCb collaboration, R. Aaij *et al.*, *LHCb detector performance*, Int. J. Mod. Phys. **A30** (2015) 1530022, arXiv:1412.6352.

[37] R. Aaij *et al.*, *Performance of the LHCb Vertex Locator*, JINST **9** (2014) P09007, arXiv:1405.7808.

[38] P. d'Argent *et al.*, *Improved performance of the LHCb Outer Tracker in LHC Run 2*, JINST **12** (2017) P11016, arXiv:1708.00819.

[39] M. Adinolfi *et al.*, *Performance of the LHCb RICH detector at the LHC*, Eur. Phys. J. **C73** (2013) 2431, arXiv:1211.6759.

[40] A. A. Alves Jr. *et al.*, *Performance of the LHCb muon system*, JINST **8** (2013) P02022, arXiv:1211.1346.

[41] R. Aaij *et al.*, *The LHCb trigger and its performance in 2011*, JINST **8** (2013) P04022, arXiv:1211.3055.

[42] F. Archilli *et al.*, *Performance of the muon identification at LHCb*, JINST **8** (2013) P10020, arXiv:1306.0249.

[43] R. Aaij *et al.*, *Performance of the LHCb trigger and full real-time reconstruction in Run 2 of the LHC*, JINST **14** (2019) P04013, arXiv:1812.10790.

[44] V. V. Gligorov and M. Williams, *Efficient, reliable and fast high-level triggering using a bonsai boosted decision tree*, JINST **8** (2013) P02013, arXiv:1210.6861.

[45] T. Sjöstrand, S. Mrenna, and P. Skands, *A brief introduction to PYTHIA 8.1*, Comput. Phys. Commun. **178** (2008) 852, arXiv:0710.3820; T. Sjöstrand, S. Mrenna, and P. Skands, *PYTHIA 6.4 physics and manual*, JHEP **05** (2006) 026, arXiv:hep-ph/0603175.

[46] I. Belyaev *et al.*, *Handling of the generation of primary events in Gauss, the LHCb simulation framework*, J. Phys. Conf. Ser. **331** (2011) 032047.

[47] C.-H. Chang, J.-X. Wang, and X.-G. Wu, *GENXICC2.0: an upgraded version of the generator for hadronic production of double heavy baryons $\Xi_{cc}$, $\Xi_{bc}$ and $\Xi_{bb}$*, Comput. Phys. Commun. **181** (2010) 1144, arXiv:0910.4462.

[48] D. J. Lange, *The EvtGen particle decay simulation package*, Nucl. Instrum. Meth. **A462** (2001) 152.

[49] P. Golonka and Z. Was, *PHOTOS Monte Carlo: A precision tool for QED corrections in Z and W decays*, Eur. Phys. J. **C45** (2006) 97, arXiv:hep-ph/0506026.

[50] Geant4 collaboration, J. Allison *et al.*, *Geant4 developments and applications*, IEEE Trans. Nucl. Sci. **53** (2006) 270; Geant4 collaboration, S. Agostinelli *et al.*, *Geant4: A simulation toolkit*, Nucl. Instrum. Meth. **A506** (2003) 250.

[51] M. Clemencic *et al.*, *The LHCb simulation application, Gauss: Design, evolution and experience*, J. Phys. Conf. Ser. **331** (2011) 032023.

[52] H. Voss, A. Hoecker, J. Stelzer, and F. Tegenfeldt, *TMVA - Toolkit for Multivariate Data Analysis with ROOT*, PoS **ACAT** (2007) 040.

[53] G. Punzi, *Sensitivity of searches for new signals and its optimization*, eConf **C030908** (2003) MODT002, arXiv:physics/0308063.

[54] T. Skwarnicki, *A study of the radiative cascade transitions between the Upsilon-prime and Upsilon resonances*, PhD thesis, Institute of Nuclear Physics, Krakow, 1986, DESY-F31-86-02.

[55] LHCb collaboration, R. Aaij *et al.*, *Measurement of the track reconstruction efficiency at LHCb*, JINST **10** (2015) P02007, arXiv:1408.1251.

[56] L. Anderlini *et al.*, *The PIDCalib package*, LHCb-PUB-2016-021, 2016.

[57] R. Aaij *et al.*, *Selection and processing of calibration samples to measure the particle identification performance of the LHCb experiment in Run 2*, EPJ Tech. Instrum. **6** (2019) 1, arXiv:1803.00824.

[58] M. Pivk and F. R. Le Diberder, *sPlot: A statistical tool to unfold data distributions*, Nucl. Instrum. Meth. **A555** (2005) 356, arXiv:physics/0402083.

[59] LHCb collaboration, R. Aaij *et al.*, *Studies of beauty baryon decays to $D^0ph^-$ and $\Lambda_c^+h^-$ final states*, Phys. Rev. **D89** (2014) 032001, arXiv:1311.4823.

[60] R. Aaij *et al.*, *The LHCb Trigger and its Performance in 2011*, JINST **8** (2013) P04022, arXiv:1211.3055.

# LHCb collaboration

R. Aaij[31], C. Abellán Beteta[49], T. Ackernley[59], B. Adeva[45], M. Adinolfi[53], H. Afsharnia[9], C.A. Aidala[83], S. Aiola[25], Z. Ajaltouni[9], S. Akar[64], J. Albrecht[14], F. Alessio[47], M. Alexander[58], A. Alfonso Albero[44], Z. Aliouche[61], G. Alkhazov[37], P. Alvarez Cartelle[47], A.A. Alves Jr[45], S. Amato[2], Y. Amhis[11], L. An[21], L. Anderlini[21], G. Andreassi[48], A. Andreianov[37], M. Andreotti[20], F. Archilli[16], A. Artamonov[43], M. Artuso[67], K. Arzymatov[41], E. Aslanides[10], M. Atzeni[49], B. Audurier[11], S. Bachmann[16], M. Bachmayer[48], J.J. Back[55], S. Baker[60], P. Baladron Rodriguez[45], V. Balagura[11,b], W. Baldini[20], J. Baptista Leite[1], R.J. Barlow[61], S. Barsuk[11], W. Barter[60], M. Bartolini[23,47,h], F. Baryshnikov[80], J.M. Basels[13], G. Bassi[28], V. Batozskaya[35], B. Batsukh[67], A. Battig[14], A. Bay[48], M. Becker[14], F. Bedeschi[28], I. Bediaga[1], A. Beiter[67], V. Belavin[41], S. Belin[26], V. Bellee[48], K. Belous[43], I. Belyaev[38], G. Bencivenni[22], E. Ben-Haim[12], A. Berezhnoy[39], R. Bernet[49], D. Berninghoff[16], H.C. Bernstein[67], C. Bertella[47], E. Bertholet[12], A. Bertolin[27], C. Betancourt[49], F. Betti[19,e], M.O. Bettler[54], Ia. Bezshyiko[49], S. Bhasin[53], J. Bhom[33], L. Bian[72], M.S. Bieker[14], S. Bifani[52], P. Billoir[12], M. Birch[60], F.C.R. Bishop[54], A. Bizzeti[21,t], M. Bjørn[62], M.P. Blago[47], T. Blake[55], F. Blanc[48], S. Blusk[67], D. Bobulska[58], V. Bocci[30], J.A. Boelhauve[14], O. Boente Garcia[45], T. Boettcher[63], A. Boldyrev[81], A. Bondar[42,w], N. Bondar[37,47], S. Borghi[61], M. Borisyak[41], M. Borsato[16], J.T. Borsuk[33], S.A. Bouchiba[48], T.J.V. Bowcock[59], A. Boyer[47], C. Bozzi[20], M.J. Bradley[60], S. Braun[65], A. Brea Rodriguez[45], M. Brodski[47], J. Brodzicka[33], A. Brossa Gonzalo[55], D. Brundu[26], A. Buonaura[49], C. Burr[47], A. Bursche[26], A. Butkevich[40], J.S. Butter[31], J. Buytaert[47], W. Byczynski[47], S. Cadeddu[26], H. Cai[72], R. Calabrese[20,g], L. Calero Diaz[22], S. Cali[22], R. Calladine[52], M. Calvi[24,i], M. Calvo Gomez[44,l], P. Camargo Magalhaes[53], A. Camboni[44], P. Campana[22], D.H. Campora Perez[47], A.F. Campoverde Quezada[5], S. Capelli[24,i], L. Capriotti[19,e], A. Carbone[19,e], G. Carboni[29], R. Cardinale[23,h], A. Cardini[26], I. Carli[6], P. Carniti[24,i], K. Carvalho Akiba[31], A. Casais Vidal[45], G. Casse[59], M. Cattaneo[47], G. Cavallero[47], S. Celani[48], R. Cenci[28], J. Cerasoli[10], A.J. Chadwick[59], M.G. Chapman[53], M. Charles[12], Ph. Charpentier[47], G. Chatzikonstantinidis[52], M. Chefdeville[8], C. Chen[3], S. Chen[26], A. Chernov[33], S.-G. Chitic[47], V. Chobanova[45], S. Cholak[48], M. Chrzaszcz[33], A. Chubykin[37], V. Chulikov[37], P. Ciambrone[22], M.F. Cicala[55], X. Cid Vidal[45], G. Ciezarek[47], P.E.L. Clarke[57], M. Clemencic[47], H.V. Cliff[54], J. Closier[47], J.L. Cobbledick[61], V. Coco[47], J.A.B. Coelho[11], J. Cogan[10], E. Cogneras[9], L. Cojocariu[36], P. Collins[47], T. Colombo[47], A. Contu[26], N. Cooke[52], G. Coombs[58], S. Coquereau[44], G. Corti[47], C.M. Costa Sobral[55], B. Couturier[47], D.C. Craik[63], J. Crkovská[66], M. Cruz Torres[1,y], R. Currie[57], C.L. Da Silva[66], E. Dall'Occo[14], J. Dalseno[45], C. D'Ambrosio[47], A. Danilina[38], P. d'Argent[47], A. Davis[61], O. De Aguiar Francisco[47], K. De Bruyn[47], S. De Capua[61], M. De Cian[48], J.M. De Miranda[1], L. De Paula[2], M. De Serio[18,d], D. De Simone[49], P. De Simone[22], J.A. de Vries[78], C.T. Dean[66], W. Dean[83], D. Decamp[8], L. Del Buono[12], B. Delaney[54], H.-P. Dembinski[14], A. Dendek[34], X. Denis[72], V. Denysenko[49], D. Derkach[81], O. Deschamps[9], F. Desse[11], F. Dettori[26,f], B. Dey[7], P. Di Nezza[22], S. Didenko[80], H. Dijkstra[47], V. Dobishuk[51], A.M. Donohoe[17], F. Dordei[26], M. Dorigo[28,x], A.C. dos Reis[1], L. Douglas[58], A. Dovbnya[50], A.G. Downes[8], K. Dreimanis[59], M.W. Dudek[33], L. Dufour[47], V. Duk[76], P. Durante[47], J.M. Durham[66], D. Dutta[61], M. Dziewiecki[16], A. Dziurda[33], A. Dzyuba[37], S. Easo[56], U. Egede[69], V. Egorychev[38], S. Eidelman[42,w], S. Eisenhardt[57], S. Ek-In[48], L. Eklund[58], S. Ely[67], A. Ene[36], E. Epple[66], S. Escher[13], J. Eschle[49], S. Esen[31], T. Evans[47], A. Falabella[19], J. Fan[3], Y. Fan[5], B. Fang[72], N. Farley[52], S. Farry[59], D. Fazzini[11], P. Fedin[38], M. Féo[47], P. Fernandez Declara[47], A. Fernandez Prieto[45], F. Ferrari[19,e], L. Ferreira Lopes[48], F. Ferreira Rodrigues[2], S. Ferreres Sole[31], M. Ferrillo[49], M. Ferro-Luzzi[47], S. Filippov[40], R.A. Fini[18], M. Fiorini[20,g], M. Firlej[34], K.M. Fischer[62], C. Fitzpatrick[61], T. Fiutowski[34], F. Fleuret[11,b], M. Fontana[47], F. Fontanelli[23,h], R. Forty[47], V. Franco Lima[59], M. Franco Sevilla[65], M. Frank[47], E. Franzoso[20],

G. Frau[16], C. Frei[47], D.A. Friday[58], J. Fu[25,p], Q. Fuehring[14], W. Funk[47], E. Gabriel[31], T. Gaintseva[41], A. Gallas Torreira[45], D. Galli[19,e], S. Gallorini[27], S. Gambetta[57], Y. Gan[3], M. Gandelman[2], P. Gandini[25], Y. Gao[4], M. Garau[26], L.M. Garcia Martin[46], P. Garcia Moreno[44], J. García Pardiñas[49], B. Garcia Plana[45], F.A. Garcia Rosales[11], L. Garrido[44], D. Gascon[44], C. Gaspar[47], R.E. Geertsema[31], D. Gerick[16], L.L. Gerken[14], E. Gersabeck[61], M. Gersabeck[61], T. Gershon[55], D. Gerstel[10], Ph. Ghez[8], V. Gibson[54], A. Gioventù[45], P. Gironella Gironell[44], L. Giubega[36], C. Giugliano[20,g], K. Gizdov[57], V.V. Gligorov[12], C. Göbel[70], E. Golobardes[44,l], D. Golubkov[38], A. Golutvin[60,80], A. Gomes[1,a], S. Gomez Fernandez[44], M. Goncerz[33], P. Gorbounov[38], I.V. Gorelov[39], C. Gotti[24,i], E. Govorkova[31], J.P. Grabowski[16], R. Graciani Diaz[44], T. Grammatico[12], L.A. Granado Cardoso[47], E. Graugés[44], E. Graverini[48], G. Graziani[21], A. Grecu[36], L.M. Greeven[31], P. Griffith[20], L. Grillo[61], L. Gruber[47], B.R. Gruberg Cazon[62], C. Gu[3], M. Guarise[20], P. A. Günther[16], E. Gushchin[40], A. Guth[13], Yu. Guz[43,47], T. Gys[47], T. Hadavizadeh[69], G. Haefeli[48], C. Haen[47], S.C. Haines[54], P.M. Hamilton[65], Q. Han[7], X. Han[16], T.H. Hancock[62], S. Hansmann-Menzemer[16], N. Harnew[62], T. Harrison[59], R. Hart[31], C. Hasse[47], M. Hatch[47], J. He[5], M. Hecker[60], K. Heijhoff[31], K. Heinicke[14], A.M. Hennequin[47], K. Hennessy[59], L. Henry[25,46], J. Heuel[13], A. Hicheur[68], D. Hill[62], M. Hilton[61], S.E. Hollitt[14], P.H. Hopchev[48], J. Hu[16], J. Hu[71], W. Hu[7], W. Huang[5], W. Hulsbergen[31], R.J. Hunter[55], M. Hushchyn[81], D. Hutchcroft[59], D. Hynds[31], P. Ibis[14], M. Idzik[34], D. Ilin[37], P. Ilten[52], A. Inglessi[37], K. Ivshin[37], R. Jacobsson[47], S. Jakobsen[47], E. Jans[31], B.K. Jashal[46], A. Jawahery[65], V. Jevtic[14], F. Jiang[3], M. John[62], D. Johnson[47], C.R. Jones[54], T.P. Jones[55], B. Jost[47], N. Jurik[62], S. Kandybei[50], Y. Kang[3], M. Karacson[47], J.M. Kariuki[53], N. Kazeev[81], M. Kecke[16], F. Keizer[54,47], M. Kelsey[67], M. Kenzie[55], T. Ketel[32], B. Khanji[47], A. Kharisova[82], S. Kholodenko[43], K.E. Kim[67], T. Kirn[13], V.S. Kirsebom[48], O. Kitouni[63], S. Klaver[31], K. Klimaszewski[35], S. Koliiev[51], A. Kondybayeva[80], A. Konoplyannikov[38], P. Kopciewicz[34], R. Kopecna[16], P. Koppenburg[31], M. Korolev[39], I. Kostiuk[31,51], O. Kot[51], S. Kotriakhova[37,30], P. Kravchenko[37], L. Kravchuk[40], R.D. Krawczyk[47], M. Kreps[55], F. Kress[60], S. Kretzschmar[13], P. Krokovny[42,w], W. Krupa[34], W. Krzemien[35], W. Kucewicz[85,33,k], M. Kucharczyk[33], V. Kudryavtsev[42,w], H.S. Kuindersma[31], G.J. Kunde[66], T. Kvaratskheliya[38], D. Lacarrere[47], G. Lafferty[61], A. Lai[26], A. Lampis[26], D. Lancierini[49], J.J. Lane[61], R. Lane[53], G. Lanfranchi[22], C. Langenbruch[13], J. Langer[14], O. Lantwin[49,80], T. Latham[55], F. Lazzari[28,u], R. Le Gac[10], S.H. Lee[83], R. Lefèvre[9], A. Leflat[39,47], S. Legotin[80], O. Leroy[10], T. Lesiak[33], B. Leverington[16], H. Li[71], L. Li[62], P. Li[16], X. Li[66], Y. Li[6], Y. Li[6], Z. Li[67], X. Liang[67], T. Lin[60], R. Lindner[47], V. Lisovskyi[14], R. Litvinov[26], G. Liu[71], H. Liu[5], S. Liu[6], X. Liu[3], A. Loi[26], J. Lomba Castro[45], I. Longstaff[58], J.H. Lopes[2], G. Loustau[49], G.H. Lovell[54], Y. Lu[6], D. Lucchesi[27,n], S. Luchuk[40], M. Lucio Martinez[31], V. Lukashenko[31], Y. Luo[3], A. Lupato[61], E. Luppi[20,g], O. Lupton[55], A. Lusiani[28,s], X. Lyu[5], L. Ma[6], S. Maccolini[19,e], F. Machefert[11], F. Maciuc[36], V. Macko[48], P. Mackowiak[14], S. Maddrell-Mander[53], L.R. Madhan Mohan[53], O. Maev[37], A. Maevskiy[81], D. Maisuzenko[37], M.W. Majewski[34], S. Malde[62], B. Malecki[47], A. Malinin[79], T. Maltsev[42,w], H. Malygina[16], G. Manca[26,f], G. Mancinelli[10], R. Manera Escalero[44], D. Manuzzi[19,e], D. Marangotto[25,p], J. Maratas[9,v], J.F. Marchand[8], U. Marconi[19], S. Mariani[21,47,21], C. Marin Benito[11], M. Marinangeli[48], P. Marino[48], J. Marks[16], P.J. Marshall[59], G. Martellotti[30], L. Martinazzoli[47], M. Martinelli[24,i], D. Martinez Santos[45], F. Martinez Vidal[46], A. Massafferri[1], M. Materok[13], R. Matev[47], A. Mathad[49], Z. Mathe[47], V. Matiunin[38], C. Matteuzzi[24], K.R. Mattioli[83], A. Mauri[31], E. Maurice[84,11,b], J. Mauricio[44], M. Mazurek[35], M. McCann[60], L. Mcconnell[17], T.H. Mcgrath[61], A. McNab[61], R. McNulty[17], J.V. Mead[59], B. Meadows[64], C. Meaux[10], G. Meier[14], N. Meinert[75], D. Melnychuk[35], S. Meloni[24,i], M. Merk[31,78], A. Merli[25], L. Meyer Garcia[2], M. Mikhasenko[47], D.A. Milanes[73], E. Millard[55], M.-N. Minard[8], L. Minzoni[20,g], S.E. Mitchell[57], B. Mitreska[61], D.S. Mitzel[47], A. Mödden[14], R.A. Mohammed[62], R.D. Moise[60], T. Mombächer[14], I.A. Monroy[73], S. Monteil[9], M. Morandin[27], G. Morello[22],

M.J. Morello[28,s], J. Moron[34], A.B. Morris[74], A.G. Morris[55], R. Mountain[67], H. Mu[3], F. Muheim[57], M. Mukherjee[7], M. Mulder[47], D. Müller[47], K. Müller[49], C.H. Murphy[62], D. Murray[61], P. Muzzetto[26], P. Naik[53], T. Nakada[48], R. Nandakumar[56], T. Nanut[48], I. Nasteva[2], M. Needham[57], I. Neri[20,g], N. Neri[25,p], S. Neubert[74], N. Neufeld[47], R. Newcombe[60], T.D. Nguyen[48], C. Nguyen-Mau[48,m], E.M. Niel[11], S. Nieswand[13], N. Nikitin[39], N.S. Nolte[47], C. Nunez[83], A. Oblakowska-Mucha[34], V. Obraztsov[43], S. Ogilvy[58], D.P. O'Hanlon[53], R. Oldeman[26,f], C.J.G. Onderwater[77], J. D. Osborn[83], A. Ossowska[33], J.M. Otalora Goicochea[2], T. Ovsiannikova[38], P. Owen[49], A. Oyanguren[46], B. Pagare[55], P.R. Pais[47], T. Pajero[28,47,s], A. Palano[18], M. Palutan[22], Y. Pan[61], G. Panshin[82], A. Papanestis[56], M. Pappagallo[57], L.L. Pappalardo[20,g], C. Pappenheimer[64], W. Parker[65], C. Parkes[61], C.J. Parkinson[45], B. Passalacqua[20], G. Passaleva[21,47], A. Pastore[18], M. Patel[60], C. Patrignani[19,e], C.J. Pawley[78], A. Pearce[47], A. Pellegrino[31], M. Pepe Altarelli[47], S. Perazzini[19], D. Pereima[38], P. Perret[9], K. Petridis[53], A. Petrolini[23,h], A. Petrov[79], S. Petrucci[57], M. Petruzzo[25], A. Philippov[41], L. Pica[28], M. Piccini[76], B. Pietrzyk[8], G. Pietrzyk[48], M. Pili[62], D. Pinci[30], J. Pinzino[47], F. Pisani[47], A. Piucci[16], Resmi P.K[10], V. Placinta[36], S. Playfer[57], J. Plews[52], M. Plo Casasus[45], F. Polci[12], M. Poli Lener[22], M. Poliakova[67], A. Poluektov[10], N. Polukhina[80,c], I. Polyakov[67], E. Polycarpo[2], G.J. Pomery[53], S. Ponce[47], A. Popov[43], D. Popov[5,47], S. Popov[41], S. Poslavskii[43], K. Prasanth[33], L. Promberger[47], C. Prouve[45], V. Pugatch[51], A. Puig Navarro[49], H. Pullen[62], G. Punzi[28,o], W. Qian[5], J. Qin[5], R. Quagliani[12], B. Quintana[8], N.V. Raab[17], R.I. Rabadan Trejo[10], B. Rachwal[34], J.H. Rademacker[53], M. Rama[28], M. Ramos Pernas[45], M.S. Rangel[2], F. Ratnikov[41,81], G. Raven[32], M. Reboud[8], F. Redi[48], F. Reiss[12], C. Remon Alepuz[46], Z. Ren[3], V. Renaudin[62], R. Ribatti[28], S. Ricciardi[56], D.S. Richards[56], K. Rinnert[59], P. Robbe[11], A. Robert[12], G. Robertson[57], A.B. Rodrigues[48], E. Rodrigues[59], J.A. Rodriguez Lopez[73], M. Roehrken[47], A. Rollings[62], P. Roloff[47], V. Romanovskiy[43], M. Romero Lamas[45], A. Romero Vidal[45], J.D. Roth[83], M. Rotondo[22], M.S. Rudolph[67], T. Ruf[47], J. Ruiz Vidal[46], A. Ryzhikov[81], J. Ryzka[34], J.J. Saborido Silva[45], N. Sagidova[37], N. Sahoo[55], B. Saitta[26,f], C. Sanchez Gras[31], C. Sanchez Mayordomo[46], R. Santacesaria[30], C. Santamarina Rios[45], M. Santimaria[22], E. Santovetti[29,j], D. Saranin[80], G. Sarpis[61], M. Sarpis[74], A. Sarti[30], C. Satriano[30,r], A. Satta[29], M. Saur[5], D. Savrina[38,39], H. Sazak[9], L.G. Scantlebury Smead[62], S. Schael[13], M. Schellenberg[14], M. Schiller[58], H. Schindler[47], M. Schmelling[15], T. Schmelzer[14], B. Schmidt[47], O. Schneider[48], A. Schopper[47], M. Schubiger[31], S. Schulte[48], M.H. Schune[11], R. Schwemmer[47], B. Sciascia[22], A. Sciubba[30], S. Sellam[68], A. Semennikov[38], A. Sergi[52,47], N. Serra[49], J. Serrano[10], L. Sestini[27], A. Seuthe[14], P. Seyfert[47], D.M. Shangase[83], M. Shapkin[43], I. Shchemerov[80], L. Shchutska[48], T. Shears[59], L. Shekhtman[42,w], V. Shevchenko[79], E.B. Shields[24,i], E. Shmanin[80], J.D. Shupperd[67], B.G. Siddi[20], R. Silva Coutinho[49], L. Silva de Oliveira[2], G. Simi[27], S. Simone[18,d], I. Skiba[20,g], N. Skidmore[74], T. Skwarnicki[67], M.W. Slater[52], J.C. Smallwood[62], J.G. Smeaton[54], A. Smetkina[38], E. Smith[13], M. Smith[60], A. Snoch[31], M. Soares[19], L. Soares Lavra[9], M.D. Sokoloff[64], F.J.P. Soler[58], A. Solovev[37], I. Solovyev[37], F.L. Souza De Almeida[2], B. Souza De Paula[2], B. Spaan[14], E. Spadaro Norella[25,p], P. Spradlin[58], F. Stagni[47], M. Stahl[64], S. Stahl[47], P. Stefko[48], O. Steinkamp[49,80], S. Stemmle[16], O. Stenyakin[43], H. Stevens[14], S. Stone[67], M.E. Stramaglia[48], M. Straticiuc[36], D. Strekalina[80], S. Strokov[82], F. Suljik[62], J. Sun[26], L. Sun[72], Y. Sun[65], P. Svihra[61], P.N. Swallow[52], K. Swientek[34], A. Szabelski[35], T. Szumlak[34], M. Szymanski[47], S. Taneja[61], Z. Tang[3], T. Tekampe[14], F. Teubert[47], E. Thomas[47], K.A. Thomson[59], M.J. Tilley[60], V. Tisserand[9], S. T'Jampens[8], M. Tobin[6], S. Tolk[47], L. Tomassetti[20,g], D. Torres Machado[1], D.Y. Tou[12], M. Traill[58], M.T. Tran[48], E. Trifonova[80], C. Trippl[48], A. Tsaregorodtsev[10], G. Tuci[28,o], A. Tully[48], N. Tuning[31], A. Ukleja[35], D.J. Unverzagt[16], A. Usachov[31], A. Ustyuzhanin[41,81], U. Uwer[16], A. Vagner[82], V. Vagnoni[19], A. Valassi[47], G. Valenti[19], M. van Beuzekom[31], H. Van Hecke[66], E. van Herwijnen[80], C.B. Van Hulse[17], M. van Veghel[77], R. Vazquez Gomez[45],

P. Vazquez Regueiro[45], C. Vázquez Sierra[31], S. Vecchi[20], J.J. Velthuis[53], M. Veltri[21,q], A. Venkateswaran[67], M. Veronesi[31], M. Vesterinen[55], D. Vieira[64], M. Vieites Diaz[48], H. Viemann[75], X. Vilasis-Cardona[44], E. Vilella Figueras[59], P. Vincent[12], G. Vitali[28], A. Vitkovskiy[31], A. Vollhardt[49], D. Vom Bruch[12], A. Vorobyev[37], V. Vorobyev[42,w], N. Voropaev[37], R. Waldi[75], J. Walsh[28], C. Wang[16], J. Wang[3], J. Wang[72], J. Wang[4], J. Wang[6], M. Wang[3], R. Wang[53], Y. Wang[7], Z. Wang[49], D.R. Ward[54], H.M. Wark[59], N.K. Watson[52], S.G. Weber[12], D. Websdale[60], C. Weisser[63], B.D.C. Westhenry[53], D.J. White[61], M. Whitehead[53], D. Wiedner[14], G. Wilkinson[62], M. Wilkinson[67], I. Williams[54], M. Williams[63,69], M.R.J. Williams[61], F.F. Wilson[56], W. Wislicki[35], M. Witek[33], L. Witola[16], G. Wormser[11], S.A. Wotton[54], H. Wu[67], K. Wyllie[47], Z. Xiang[5], D. Xiao[7], Y. Xie[7], H. Xing[71], A. Xu[4], J. Xu[5], L. Xu[3], M. Xu[7], Q. Xu[5], Z. Xu[5], Z. Xu[4], D. Yang[3], Y. Yang[5], Z. Yang[3], Z. Yang[65], Y. Yao[67], L.E. Yeomans[59], H. Yin[7], J. Yu[7], X. Yuan[67], O. Yushchenko[43], K.A. Zarebski[52], M. Zavertyaev[15,c], M. Zdybal[33], O. Zenaiev[47], M. Zeng[3], D. Zhang[7], L. Zhang[3], S. Zhang[4], Y. Zhang[47], A. Zhelezov[16], Y. Zheng[5], X. Zhou[5], Y. Zhou[5], X. Zhu[3], V. Zhukov[13,39], J.B. Zonneveld[57], S. Zucchelli[19,e], D. Zuliani[27], G. Zunica[61].

[1] *Centro Brasileiro de Pesquisas Físicas (CBPF), Rio de Janeiro, Brazil*
[2] *Universidade Federal do Rio de Janeiro (UFRJ), Rio de Janeiro, Brazil*
[3] *Center for High Energy Physics, Tsinghua University, Beijing, China*
[4] *School of Physics State Key Laboratory of Nuclear Physics and Technology, Peking University, Beijing, China*
[5] *University of Chinese Academy of Sciences, Beijing, China*
[6] *Institute Of High Energy Physics (IHEP), Beijing, China*
[7] *Institute of Particle Physics, Central China Normal University, Wuhan, Hubei, China*
[8] *Univ. Grenoble Alpes, Univ. Savoie Mont Blanc, CNRS, IN2P3-LAPP, Annecy, France*
[9] *Université Clermont Auvergne, CNRS/IN2P3, LPC, Clermont-Ferrand, France*
[10] *Aix Marseille Univ, CNRS/IN2P3, CPPM, Marseille, France*
[11] *Université Paris-Saclay, CNRS/IN2P3, IJCLab, Orsay, France*
[12] *LPNHE, Sorbonne Université, Paris Diderot Sorbonne Paris Cité, CNRS/IN2P3, Paris, France*
[13] *I. Physikalisches Institut, RWTH Aachen University, Aachen, Germany*
[14] *Fakultät Physik, Technische Universität Dortmund, Dortmund, Germany*
[15] *Max-Planck-Institut für Kernphysik (MPIK), Heidelberg, Germany*
[16] *Physikalisches Institut, Ruprecht-Karls-Universität Heidelberg, Heidelberg, Germany*
[17] *School of Physics, University College Dublin, Dublin, Ireland*
[18] *INFN Sezione di Bari, Bari, Italy*
[19] *INFN Sezione di Bologna, Bologna, Italy*
[20] *INFN Sezione di Ferrara, Ferrara, Italy*
[21] *INFN Sezione di Firenze, Firenze, Italy*
[22] *INFN Laboratori Nazionali di Frascati, Frascati, Italy*
[23] *INFN Sezione di Genova, Genova, Italy*
[24] *INFN Sezione di Milano-Bicocca, Milano, Italy*
[25] *INFN Sezione di Milano, Milano, Italy*
[26] *INFN Sezione di Cagliari, Monserrato, Italy*
[27] *Universita degli Studi di Padova, Universita e INFN, Padova, Padova, Italy*
[28] *INFN Sezione di Pisa, Pisa, Italy*
[29] *INFN Sezione di Roma Tor Vergata, Roma, Italy*
[30] *INFN Sezione di Roma La Sapienza, Roma, Italy*
[31] *Nikhef National Institute for Subatomic Physics, Amsterdam, Netherlands*
[32] *Nikhef National Institute for Subatomic Physics and VU University Amsterdam, Amsterdam, Netherlands*
[33] *Henryk Niewodniczanski Institute of Nuclear Physics Polish Academy of Sciences, Kraków, Poland*
[34] *AGH - University of Science and Technology, Faculty of Physics and Applied Computer Science, Kraków, Poland*
[35] *National Center for Nuclear Research (NCBJ), Warsaw, Poland*
[36] *Horia Hulubei National Institute of Physics and Nuclear Engineering, Bucharest-Magurele, Romania*

[37] *Petersburg Nuclear Physics Institute NRC Kurchatov Institute (PNPI NRC KI), Gatchina, Russia*
[38] *Institute of Theoretical and Experimental Physics NRC Kurchatov Institute (ITEP NRC KI), Moscow, Russia, Moscow, Russia*
[39] *Institute of Nuclear Physics, Moscow State University (SINP MSU), Moscow, Russia*
[40] *Institute for Nuclear Research of the Russian Academy of Sciences (INR RAS), Moscow, Russia*
[41] *Yandex School of Data Analysis, Moscow, Russia*
[42] *Budker Institute of Nuclear Physics (SB RAS), Novosibirsk, Russia*
[43] *Institute for High Energy Physics NRC Kurchatov Institute (IHEP NRC KI), Protvino, Russia, Protvino, Russia*
[44] *ICCUB, Universitat de Barcelona, Barcelona, Spain*
[45] *Instituto Galego de Física de Altas Enerxías (IGFAE), Universidade de Santiago de Compostela, Santiago de Compostela, Spain*
[46] *Instituto de Fisica Corpuscular, Centro Mixto Universidad de Valencia - CSIC, Valencia, Spain*
[47] *European Organization for Nuclear Research (CERN), Geneva, Switzerland*
[48] *Institute of Physics, Ecole Polytechnique Fédérale de Lausanne (EPFL), Lausanne, Switzerland*
[49] *Physik-Institut, Universität Zürich, Zürich, Switzerland*
[50] *NSC Kharkiv Institute of Physics and Technology (NSC KIPT), Kharkiv, Ukraine*
[51] *Institute for Nuclear Research of the National Academy of Sciences (KINR), Kyiv, Ukraine*
[52] *University of Birmingham, Birmingham, United Kingdom*
[53] *H.H. Wills Physics Laboratory, University of Bristol, Bristol, United Kingdom*
[54] *Cavendish Laboratory, University of Cambridge, Cambridge, United Kingdom*
[55] *Department of Physics, University of Warwick, Coventry, United Kingdom*
[56] *STFC Rutherford Appleton Laboratory, Didcot, United Kingdom*
[57] *School of Physics and Astronomy, University of Edinburgh, Edinburgh, United Kingdom*
[58] *School of Physics and Astronomy, University of Glasgow, Glasgow, United Kingdom*
[59] *Oliver Lodge Laboratory, University of Liverpool, Liverpool, United Kingdom*
[60] *Imperial College London, London, United Kingdom*
[61] *Department of Physics and Astronomy, University of Manchester, Manchester, United Kingdom*
[62] *Department of Physics, University of Oxford, Oxford, United Kingdom*
[63] *Massachusetts Institute of Technology, Cambridge, MA, United States*
[64] *University of Cincinnati, Cincinnati, OH, United States*
[65] *University of Maryland, College Park, MD, United States*
[66] *Los Alamos National Laboratory (LANL), Los Alamos, United States*
[67] *Syracuse University, Syracuse, NY, United States*
[68] *Laboratory of Mathematical and Subatomic Physics , Constantine, Algeria, associated to* [2]
[69] *School of Physics and Astronomy, Monash University, Melbourne, Australia, associated to* [55]
[70] *Pontifícia Universidade Católica do Rio de Janeiro (PUC-Rio), Rio de Janeiro, Brazil, associated to* [2]
[71] *Guangdong Provencial Key Laboratory of Nuclear Science, Institute of Quantum Matter, South China Normal University, Guangzhou, China, associated to* [3]
[72] *School of Physics and Technology, Wuhan University, Wuhan, China, associated to* [3]
[73] *Departamento de Fisica , Universidad Nacional de Colombia, Bogota, Colombia, associated to* [12]
[74] *Universität Bonn - Helmholtz-Institut für Strahlen und Kernphysik, Bonn, Germany, associated to* [16]
[75] *Institut für Physik, Universität Rostock, Rostock, Germany, associated to* [16]
[76] *INFN Sezione di Perugia, Perugia, Italy, associated to* [20]
[77] *Van Swinderen Institute, University of Groningen, Groningen, Netherlands, associated to* [31]
[78] *Universiteit Maastricht, Maastricht, Netherlands, associated to* [31]
[79] *National Research Centre Kurchatov Institute, Moscow, Russia, associated to* [38]
[80] *National University of Science and Technology "MISIS", Moscow, Russia, associated to* [38]
[81] *National Research University Higher School of Economics, Moscow, Russia, associated to* [41]
[82] *National Research Tomsk Polytechnic University, Tomsk, Russia, associated to* [38]
[83] *University of Michigan, Ann Arbor, United States, associated to* [67]
[84] *Laboratoire Leprince-Ringuet, Palaiseau, France*
[85] *AGH - University of Science and Technology, Faculty of Computer Science, Electronics and Telecommunications, Kraków, Poland*

[a] *Universidade Federal do Triângulo Mineiro (UFTM), Uberaba-MG, Brazil*
[b] *Laboratoire Leprince-Ringuet, Palaiseau, France*

[c] *P.N. Lebedev Physical Institute, Russian Academy of Science (LPI RAS), Moscow, Russia*
[d] *Università di Bari, Bari, Italy*
[e] *Università di Bologna, Bologna, Italy*
[f] *Università di Cagliari, Cagliari, Italy*
[g] *Università di Ferrara, Ferrara, Italy*
[h] *Università di Genova, Genova, Italy*
[i] *Università di Milano Bicocca, Milano, Italy*
[j] *Università di Roma Tor Vergata, Roma, Italy*
[k] *AGH - University of Science and Technology, Faculty of Computer Science, Electronics and Telecommunications, Kraków, Poland*
[l] *DS4DS, La Salle, Universitat Ramon Llull, Barcelona, Spain*
[m] *Hanoi University of Science, Hanoi, Vietnam*
[n] *Università di Padova, Padova, Italy*
[o] *Università di Pisa, Pisa, Italy*
[p] *Università degli Studi di Milano, Milano, Italy*
[q] *Università di Urbino, Urbino, Italy*
[r] *Università della Basilicata, Potenza, Italy*
[s] *Scuola Normale Superiore, Pisa, Italy*
[t] *Università di Modena e Reggio Emilia, Modena, Italy*
[u] *Università di Siena, Siena, Italy*
[v] *MSU - Iligan Institute of Technology (MSU-IIT), Iligan, Philippines*
[w] *Novosibirsk State University, Novosibirsk, Russia*
[x] *INFN Sezione di Trieste, Trieste, Italy*
[y] *Universidad Nacional Autonoma de Honduras, Tegucigalpa, Honduras*